RESEARCH ARTICLE

Indeno[1,2,3,4-*pqra*]perylene: A Medium-Sized Aromatic Hydrocarbon Exhibiting Full-Range Visible-Light Absorption

Masaki Kato,[a] Norihito Fukui,*[a,b] and Hiroshi Shinokubo*[a]

[a] M. Kato, Dr. N. Fukui, Prof. Dr. H. Shinokubo
Department of Molecular and Macromolecular Chemistry, Graduate School of Engineering
Nagoya University
Furo-cho, Chikusa-ku, Nagoya 464-8603 (Japan)
E-mail: fukui@chembio.nagoya-u.ac.jp, hshino@chembio.nagoya-u.ac.jp
[b] Dr. N. Fukui
PRESTO, Japan Science and Technology Agency (JST)
Kawaguchi, Saitama 332-0012 (Japan)

Supporting information for this article is given via a link at the end of the document.

Abstract: We report the synthesis and properties of indeno[1,2,3,4-*pqra*]perylene, which was prepared by the fusion of one anthracene unit with one naphthalene unit via three carbon–carbon bonds. The synthetic route through two-fold C–H arylation enabled not only the synthesis of unsubstituted indenoperylene, but also rapid access to its arylated derivatives on the gram scale. Indenoperylene is a medium-sized aromatic hydrocarbon with the composition $C_{24}H_{12}$ that is isomeric to coronene. Nevertheless, its absorption covers the entire visible region owing to its small HOMO–LUMO gap. Furthermore, indenoperylene exhibits high stability despite the absence of peripheral substituents. We propose that the unique electronic structure of indenoperylene originates from the coexistence of an electron-withdrawing subunit (benzoaceanthrylene) and an electron-donating subunit (perylene). The electronic properties of indenoperylene were modulated via post-functionalization through regioselective bromination. The current research demonstrates that indenoperylene is a promising candidate as a main skeleton for near-infrared-responsive and redox-active materials.

Introduction

Carbon and hydrogen are fundamental components of organic molecules. Various functional π-systems have been designed via the structural modification of conventional aromatic hydrocarbons. Novel aromatic hydrocarbon skeletons with attractive electronic structures are a source of novel functional materials. Notably, conjugated hydrocarbons with a narrow HOMO–LUMO gap are attractive research targets.[1–4] These molecules exhibit intriguing properties, including near-infrared (NIR) absorption, reversible redox activity, and high single-molecule conductance, making them promising candidates for various practical applications including organic (semi)conductors, NIR-responsive dyes, and rechargeable batteries.

Hydrocarbons with antiaromaticity or diradical character often exhibit a narrow HOMO–LUMO gap.[5–20] However, these molecules are inherently reactive, and thus require kinetic stabilization by sterically hindered peripheral substituents. These bulky substituents usually hamper their electronic modulation by peripheral functionalization. Moreover, they also prevent effective intermolecular interactions in the condensed phases, making this approach unsuitable for the fabrication of solid-state materials.

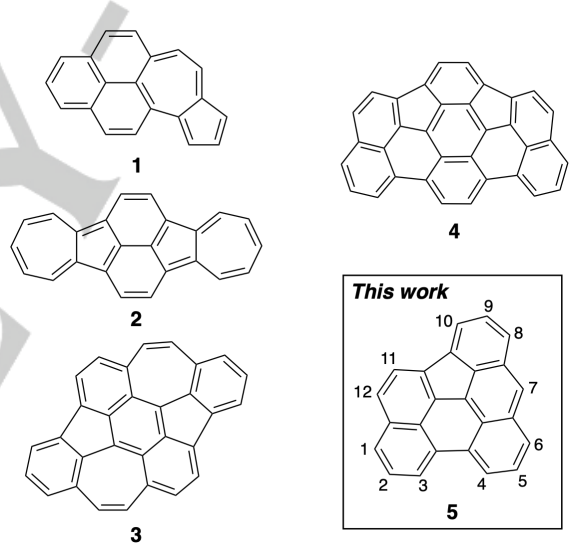

Figure 1. Representative nonalternant hydrocarbons (**1**–**5**) that exhibit narrow HOMO–LUMO gaps without stabilization by peripheral substituents.

The incorporation of nonalternant hydrocarbon[21,22] segments should be an effective approach to circumvent the aforementioned obstacles. While the majority of nonalternant hydrocarbons exhibit antiaromaticity and/or diradical character, and thus require kinetic stabilization,[5-16] several exceptional examples with no peripheral substituents have been reported.[23–28] In 1977, Murata and co-workers synthesized azulenophenalene **1**, which exhibits an absorption peak at 900 nm (Figure 1).[23] Ito and co-workers reported that the absorption of naphthodiazulene **2** reached 1400 nm.[25] The group of Zhang recently synthesized the azulene-incorporating polycyclic aromatic hydrocarbon (PAH) **3**, whose absorption covers the entire visible region.[26] Our group also recently contributed to this research field, demonstrating that *as*-indacenoterrylene **4** displayed NIR-absorption tailing to ca. 1300 nm.[28] Curiously, **4** exhibits negligible antiaromaticity and diradical character. We

tentatively attributed the absorption features of **4** to the coexistence of an electron-withdrawing subunit and an electron-donating subunit. This concept should be promising as a rational approach to reconcile the narrow HOMO–LUMO gap with the stability of a molecule. In the present study, we report on the synthesis and properties of indeno[1,2,3,4-*pqra*]perylene **5**, which contains both an electron-withdrawing subunit (benzoaceanthrylene) and an electron-donating subunit (perylene).

Results and Discussion

The synthetic route to indenoperylene **5** is shown in Scheme 1. The bromine–lithium exchange reaction of 1-bromonaphthalene with butyllithium, followed by the addition of 1,8-dichloroanthracen-9-(10*H*)-one (**6**)[29] afforded the corresponding naphthylated alcohol **7** in 20% yield. Treatment of **7** with sodium hydride (NaH) provided 1,8-dichloro-9-(1-naphthyl)anthracene (**8**) in 43% yield via dehydration. The intramolecular double C–H/C–Cl coupling[30] of **8** in the presence of palladium acetate ($Pd(OAc)_2$), pivalic acid (PivOH), tricyclohexylphosphonium tetrafluoroborate ($PCy_3{\cdot}HBF_4$), and potassium carbonate (K_2CO_3) furnished indenoperylene **5** in 45% yield. This yield is rather high considering the relatively high strain in the indenoperylene skeleton (*vide infra*). The reaction also provided naphtho[1,2-*a*]aceanthrylene **9** in 9% yield, which was formed by the dechlorination of a singly-coupled intermediate.

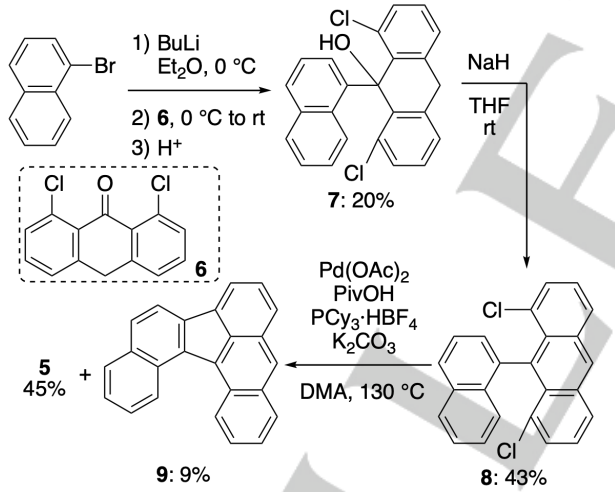

Scheme 1. Synthesis of indenoperylene **5**.

Then, we examined the thermal stability of **5** in a 1,2-dichlorobenzene solution at 180 °C for 24 h under aerobic conditions by monitoring its absorption (Figure S69). The absorption spectra remained almost constant, confirming the high stability of **5** despite the absence of peripheral substituents.

We also synthesized peripherally functionalized derivatives (Scheme 2). 1,8-Dichloro-9-(naphthalen-1-yl)-10-(4-methylphenyl)anthracene **10a** and 1,8-dichloro-9-(naphthalen-1-yl)-10-(3,5-di-*tert*-butylphenyl)anthracene **10b** were prepared from commercially available 1,8-dichloroanthraquinone via four-step transformations with total yields of 18% and 13%, respectively (for details, see the Supporting Information). **10a** and **10b** were then subjected to an intramolecular C–H/C–Cl coupling reaction, which afforded 7-(4-methylphenyl)indenoperylene **11a** and 7-(3,5-di-*tert*-butylphenyl)indenoperylene **11b** in 60% and 77% yields, respectively. Importantly, this reaction is scalable and allows the large-scale preparation of **11b** on the gram scale.

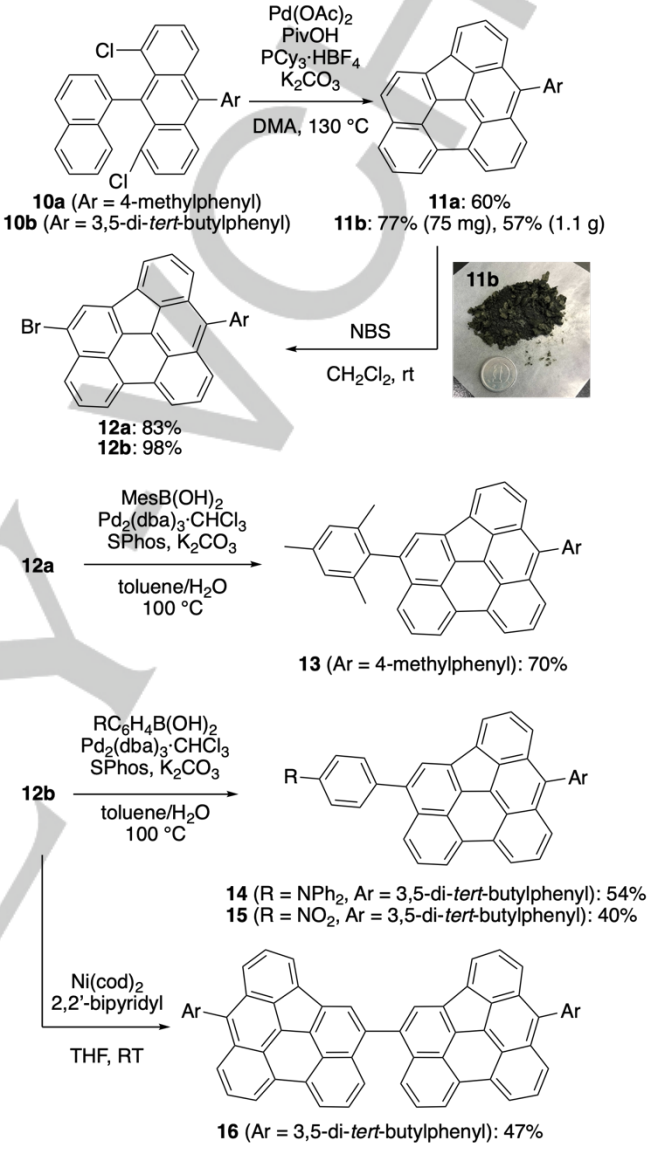

Scheme 2. Synthesis of peripherally functionalized indenoperylenes.

The bromination of **11a** and **11b** with *N*-bromosuccinimide (NBS) proceeded selectively at the 12-position to afford **12a** and **12b** in 83% and 98% yield, respectively (Scheme 2). The Suzuki–Miyaura cross-coupling reaction of **12a** with mesitylboronic acid furnished 12-mesityl-7-(4-methylphenyl)indenoperylene **13** in 70% yield despite the steric bulk of the substituent. Both electron-donating and electron-withdrawing aryl groups were compatible, as 12-(4-diphenylaminophenyl) derivative **14** and 12-(4-nitrophenyl) derivative **15** were obtained in 54% and 40% yields, respectively. The nickel-mediated Yamamoto coupling of **12b** furnished 12,12′-linked dimer **16** in 47% yield. These results highlight that indenoperylene is suitable for late-stage functionalizations that enable the creation of elaborate π-systems.

The structure of 12-mesityl-7-(4-methylphenyl)indenoperylene **13** was unambiguously determined by single-crystal X-ray diffraction analysis (Figure 2).[31] The unit cell includes two crystallographically independent molecules, both of which exhibit similar structural features. One of these is shown in Figure 2. The indenoperylene fragment of **13** is planar with a small mean plane deviation (MPD = 0.042 Å). The C(1)–C(2) bond located at the center (1.396(5) Å) is shorter than that of a typical C(sp^2)–C(sp^2) bond (1.44 Å) and comparable to the C–C bond length of benzene (1.40 Å). In contrast, the C(3)–C(4) bond at the outer-bay region is relatively long (1.501(5) Å). The maximum and minimum bond angles of the five six-membered rings are 128° and 113°, respectively. These features emphasize the significant distortion in the structure. The harmonic oscillator model of aromaticity (HOMA) values at the five six-membered rings are comparable to those of the fragments of indenoperylene, namely naphthalene, anthracene, and perylene (Figure S60).[32] These results suggest the negligible effect of structural distortion on the degree of aromaticity given the structural criteria.

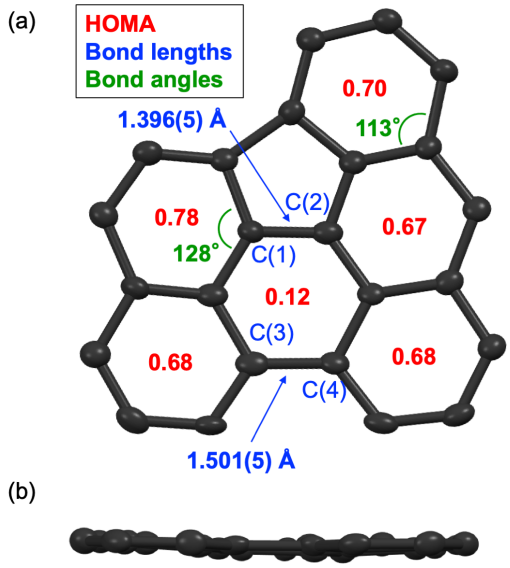

Figure 2. X-ray crystal structure of **13**. (a) Top and (b) side views. Thermal ellipsoids are shown at 50% probability. All hydrogen atoms, the 4-methylphenyl group, and the mesityl group are omitted for clarity.

The UV/vis absorption spectra of indenoperylene **5**, naphthoaceanthrylene **9**, 12-mesityl-7-(4-methylphenyl)indenoperylene **13**, 12-(4-diphenylaminophenyl) derivative **14**, 12-(4-nitrophenyl) derivative **15**, 12,12'-linked dimer **16**, and coronene are shown in Figure 3. Importantly, the low-energy absorption of **5** reaches 680 nm, which covers the entire visible region. This result highlights the remarkable light-harvesting ability of **5**. The absorption of **5** is more red-shifted than that of coronene (up to ca. 360 nm) although coronene is a structural isomer of **5**. The absorption of **5** is accompanied by vibrational bands, suggesting structural rigidity. It is worth noting that no emission was observed for **5** in the range of 400–1150 nm. The absorption of **9** is significantly blue-shifted by ca. 2.5 × 10^3 cm^{-1} relative to that of **5**, which indicates the effective π-conjugation through the C(3)–C(4) bond of **5**. The absorption of **5** obeys the Lambert–Beer law (Figure S70). The absorption features of **5** are essentially the same as those of the corresponding aryl-substituted derivative **13**. These results clearly suggest that the full-range visible-light absorption is not due to aggregation. The slight red-shift of the absorption of **13** compared to that of **5** is likely due to the electronic delocalization on the substituents. 12-(4-Diphenylaminophenyl) derivative **14**, 12-(4-nitrophenyl) derivative **15**, and 12,12′ -linked dimer **16** exhibit more red-shifted absorption spectra relative to that of **5**, tailing to ca. 730–750 nm. These results indicate that the electronic properties of indenoperylene are tunable via peripheral functionalization.

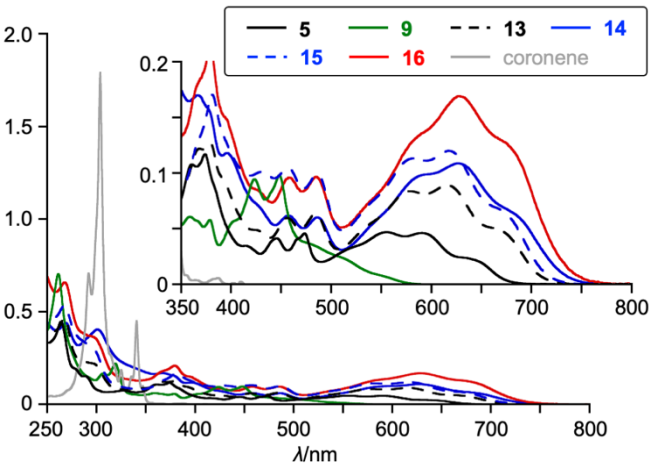

Figure 3. UV/vis absorption spectra of **5**, **9**, **13**, **14**, **15**, **16**, and coronene in CH_2Cl_2; λ: wavelength; ε: extinction coefficient.

The cyclic voltammograms of **5**, **11b**, **14**, **15**, and **16** were measured in CH_2Cl_2 (Figures S61, S62; Table 1). The ferrocene/ferrocenium couple (Fc/Fc^+) was used as an external reference. Indenoperylene **5** exhibited one reversible oxidation wave at 0.39 V and one reversible reduction wave at –1.65 V. 7-Arylated derivative **11b** exhibited similar redox potentials. 12-(4-Diphenylaminophenyl) derivative **14** and 12,12′ -linked dimer **16** showed lower first oxidation potentials of 0.27 and 0.22 V, respectively. 12-(4-Nitrophenyl) derivative **15** showed a higher first reduction potential of 1.51 V. Dimer **16** exhibited a large split between the first and second oxidation potentials (0.27 V), indicating effective electronic interaction between the indenoperylene subunits.

Table 1. Redox potentials of **5**, **11b**, **14**, **15**, and **16**[a]

	Reduction [V]	Oxidation [V]		ΔE[b] [eV]
	E_{red1}	E_{ox1}	E_{ox2}	
5	–1.65	0.39	—	2.04
11b	–1.67	0.44	—	2.11
14	-1.64	0.27	0.46	1.91
15	-1.51	0.47	—	1.98
16	-1.66	0.22	0.49	1.88

[a] Redox potentials were measured via cyclic voltammetry in anhydrous CH_2Cl_2 using 0.1 M $[Bu_4N][PF_6]$ as the supporting electrolyte and $Ag/AgNO_3$ as the

reference electrode. The ferrocene/ferrocenium ion couple was used as an external reference. [b] Electrochemical HOMO–LUMO gap ($\Delta E = E_{ox1} - E_{red1}$).

To understand the electronic structure of indenoperylene **5**, density functional theory (DFT) calculations were conducted at the B3LYP/6-31G(d) level of theory (Figure S63–S67). The calculated HOMO and LUMO of **5** are shown in Figure 4. The calculated HOMO–LUMO gap of **5** (2.42 eV) is significantly smaller than that of coronene (4.04 eV) despite both having the same composition ($C_{24}H_{12}$). The HOMO and LUMO of **5** are mainly delocalized on the perylene-like and benzoaceanthrylene-like moieties, respectively. Their energy levels (HOMO: –4.89 eV; LUMO: –2.47 eV) agree well with those of the fragments of **5** (HOMO of perylene: –4.95 eV; LUMO of benzoaceanthrylene: –2.60 eV), respectively. Consequently, we attribute the narrow HOMO–LUMO gap of **5** to the coexistence of an electron-donating and an electron-withdrawing subunit in a single molecular skeleton. This rationale is also valid for indacenoterrylene **4**. We also conducted time-dependent (TD)-DFT calculations, which nicely reproduced the absorption of **5** (Figure S68). The calculations predict that [HOMO]–[LUMO] transition (86%) and [HOMO–1]–[LUMO] transition (14%) contribute to the lowest-energy absorption.

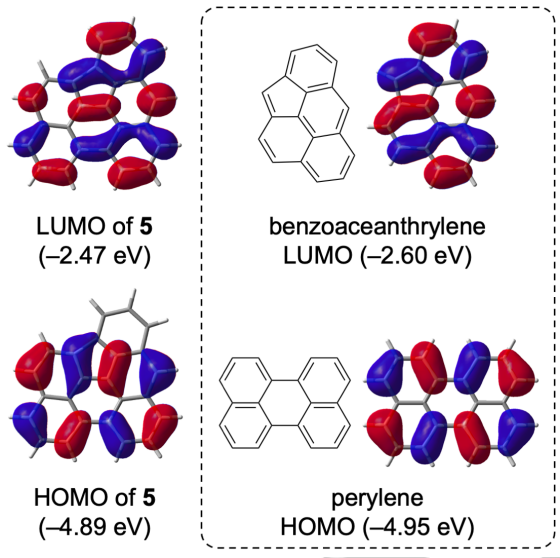

Figure 4. Molecular frontier orbital representations of **5**, benzoaceanthrylene, and perylene. Calculations were performed at the B3LYP/6-31G(d) level of theory (isovalue = 0.02).

Then, we also evaluated the aromaticity and diradical character of **5**. The ^{1}H NMR signals of **5** were observed in the region diagnostic for aromatic molecules (8.20–7.47 ppm). Nucleus-independent chemical shift (NICS)[33,34] calculations suggested that the six-membered rings of fused naphthalene and anthracene fragments exhibit local benzene-like aromaticity (Figure 5a). The NICS(1)$_{zz}$ values of **5** are comparable to those of its fragments perylene and benzoaceanthrylene. The anisotropy of the induced current density (ACID)[35] plot shows that the main ring currents are diatropic, and circulate around the naphthalene and anthracene segments, respectively (Figure 5b). These results indicate that the contribution of macrocyclic antiaromaticity to the properties of **5** is negligible. Calculations of **5** at the CASSCF(2,2)/6-31G(d) level of theory afforded a diradical index *y* of 0.06. Broken-symmetry DFT calculations at the (U)B3LYP/6-31G(d) and (U)BHandHLYP/6-31G(d) levels of theory furnished diradical indexes of zero and 0.04, respectively. These results negate the contribution of the diradical character to the electronic structure of indenoperylene.

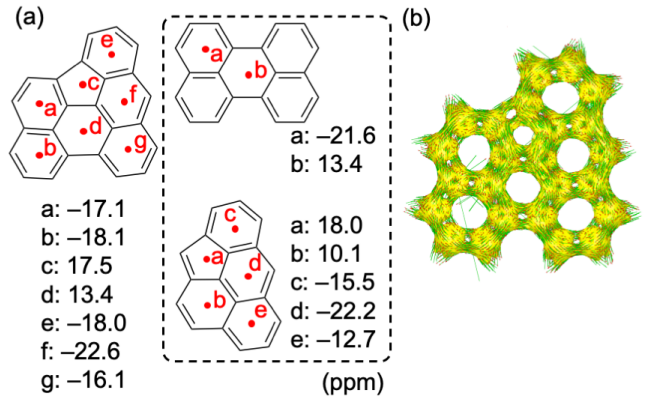

Figure 5. (a) NICS(1)$_{zz}$ values (ppm) of **5**, perylene, and benzoace-anthrylene. (b) ACID plot of **5**. All calculations were conducted at the B3LYP/6-31G(d) level of theory.

Conclusion

We have described the synthesis and properties of indenoperylene **5** and its 9-arylated derivatives **11a** and **11b**. These compounds were prepared via the intramolecular double C–H/C–Cl coupling of the corresponding 1,8-dichloro-9-(1-naphthyl)anthracenes in good yield (45–77%) and excellent scalability (up to 1.1 g). The structure of mesityl derivative **13** was confirmed via single-crystal X-ray diffraction analysis. The indenoperylene skeleton was planar despite the presence of a fused five-membered ring, albeit that the constituent six-membered rings were significantly contorted. Importantly, the absorption of indenoperylene covered the entire visible region despite its rather small π-conjugated system. The narrow HOMO–LUMO gap of **5** was further supported by electrochemical measurement and theoretical calculations. Indenoperylene **5** exhibited high stability despite its lack of peripheral substituents. DFT calculations suggested negligible contributions of antiaromaticity and diradical character to the electronic properties of **5**. The current research demonstrates that indenoperylene is a promising candidate as a main skeleton for various functional materials including organic semiconductors, NIR-responsive dyes, and rechargeable batteries.

Acknowledgements

This work was supported by JSPS KAKENHI grants JP20H05863, JP20K15257, and JP20H05867 as well as JST, PRESTO Grant Number JPMJPR21Q7, Japan. N. F. gratefully acknowledges the Mitsubishi Foundation and Toyota Physical and Chemical Research Institute for financial support. The authors acknowledge Prof. Dr. Shigehiro Yamaguchi, Dr. Soichiro Ogi, and Ms. Natsumi Fukaya for NIR emission measurement.

Keywords: polycyclic aromatic hydrocarbon • full-range visible-light absorption • narrow HOMO–LUMO gap • nonalternant hydrocarbon • CH arylation

[1] Z. Sun, Q. Ye, C. Chi, J. Wu, *Chem. Soc. Rev.* **2012**, *41*, 7857–7889.
[2] H. Hopf, *Angew. Chem. Int. Ed.* **2013**, *52*, 12224–12226; *Angew. Chem.* **2013**, *125*, 12446–12449.
[3] T. Kubo, *Chem. Rec.* **2015**, *15*, 218–232.
[4] X. Hu, W. Wang, D. Wang, Y. Zheng, *J. Mater. Chem. C* **2018**, *6*, 11232–11242.
[5] G. E. Rudebusch, J. L. Zafra, K. Jorner, K. Fukuda, J. L. Marshall, I. Arrechea-Marcos, G. L. Espejo, R. P. Ortiz, C. J. Gómez-García, L. N. Zakharov, M. Nakano, H. Ottosson, J. Casado, M. M. Haley, *Nat. Chem.* **2016**, *8*, 753–759.
[6] C. K. Frederickson, B. D. Rose, M. M. Haley, *Acc. Chem. Res.* **2017**, *50*, 977–987.
[7] A. Shimidzu, Y. Tobe, Indeno[2,1-*a*]fluorene: An Air-Stable *ortho*-Quinodimethane Derivative. *Angew. Chem. Int. Ed.* **2011**, *50*, 6906–6910; *Angew. Chem.* **2011**, *123*, 7038–7042
[8] S. Nobusue, H. Miyoshi, A. Shimizu, I. Hisaki, K. Fukuda, M. Nakano, Y. Tobe, *Angew. Chem. Int. Ed.* **2015**, *54*, 2090–2094; *Angew. Chem.* **2015**, *127*, 2118–2122.
[9] Y. Zou, W. Zeng, T. Y. Gopalakrishna, Y. Han, Q. Jiang, J. Wu, *J. Am. Chem. Soc.* **2019**, *141*, 7266–7270.
[10] T. Kawase, T. Fujiwara, C. Kitamura, A. Konishi, Y. Hirao, K. Matsumoto, H. Kurata, T. Kubo, S. Shinomura, H. Mori, E. Miyazaki, K. Takimiya, *Angew. Chem. Int. Ed.* **2010**, *49*, 7728–7732; *Angew. Chem.* **2010**, *122*, 7894–7898.
[11] A. Konishi, Y. Okada, M. Nakano, K. Sugisaki, K. Sato, T. Takui, M. Yasuda, *J. Am. Chem. Soc.* **2017**, *139*, 15284–15287.
[12] A. Konishi, Y. Okada, R. Kishi, M. Nakano, M. Yasuda, *J. Am. Chem. Soc.* **2019**, *141*, 560–571.
[13] A. Konishi, K. Horii, D. Shiomi, K. Sato, T. Takui, M. Yasuda, *J. Am. Chem. Soc.* **2019**, *141*, 10165–10170.
[14] H. Oshima, A. Fukazawa, S. Yamaguchi, *Angew. Chem. Int. Ed.* **2017**, *56*, 3270–3274; *Angew. Chem.* **2017**, *129*, 3318–3322.
[15] R.-Q. Lu, S. Wu, L.-L. Yang, W.-B. Gao, H. Qu, X.-Y. Wang, J.-B. Chen, C. Tang, H.-Y. Shi, X.-Y. Cao, *Angew. Chem. Int. Ed.* **2019**, *58*, 7600–7605; *Angew. Chem.* **2019**, *131*, 7682–7687.
[16] Y.-C. Hsieh, C.-F. Wu, Y.-T. Chen, C.-T. Fang, C.-S. Wang, C.-H. Li, L.-Y. Chen, M.-J. Cheng, C.-C. Chueh, P.-T. Chou, Y.-T.; Wu, *J. Am. Chem. Soc.* **2018**, *140*, 14357–14366.
[17] T. Kubo, A. Shimizu, M. Sakamoto, M. Uruichi, K. Yakushi, M. Nakano, D. Shiomi, K. Sato, T. Takui, Y. Morita, K. Nakasuji, *Angew. Chem. Int. Ed.* **2005**, *44*, 6564–6568; *Angew. Chem.* **2005**, *117*, 6722–6726.
[18] A. Konishi, Y. Hirao, M. Nakano, A. Shimizu, E. Botek, B. Champagne, D. Shiomi, K. Sato, T. Takui, K. Matsumoto, H. Kurata, T. Kubo, *J. Am. Chem. Soc.* **2010**, *132*, 11021–11023.
[19] Y. Ni, T. Y. Gopalakrishna, H. Phan, T. S. Herng, S. Wu, Y. Han, J. Ding, J. Wu, *Angew. Chem. Int. Ed.* **2018**, *57*, 9697–9701; *Angew. Chem.* **2018**, *130*, 9845–9849.
[20] W. Zeng, T. Y. Gopalakrishna, H. Phan, T. Tanaka, T. S. Herng, J. Ding, A. Osuka, J. Wu, *J. Am. Chem. Soc.* **2018**, *140*, 14054–14058.
[21] Y. Tobe, *Chem. Rec.* **2015**, *15*, 86–96.
[22] K. Hafner, *Angew. Chem. Int. Ed. Engl.* **1964**, *3*, 165–173.
[23] K. Nakasuji, E. Todo, I. Murata, *Angew. Chem. Int. Ed. Engl.* **1977**, *16*, 784–785.
[24] E. Todo, K. Yamamoto, I. Murata, *Chem. Lett.* **1979**, *8*, 537–540.
[25] Y. Fukazawa, M. Aoyagi, S. Itô, *Tetrahedron Lett.* **1981**, *22*, 3879–3882.
[26] X.-S. Zhang, Y.-Y. Huang, J. Zhang, W. Meng, Q. Peng, R. Kong, Z. Xiao, J. Liu, M. Huang, Y. Yi, L. Chen, Q. Fan, G. Lin, Z. Liu, G. Zhang, L. Jiang, D. Zhang, *Angew. Chem. Int. Ed.* **2020**, *59*, 3529–3533; *Angew. Chem.* **2020**, *132*, 3557–3561.
[27] X. Yang, F. Rominger, M. Mastalerz, *Angew. Chem. Int. Ed.* **2019**, *58*, 17577–17582; *Angew. Chem.* **2019**, *131*, 17741–17746.
[28] Y. Tanaka, N. Fukui, H. Shinokubo, *Nat. Commun.* **2020**, *11*, 3873.
[29] H. O. House, N. I. Ghali, J. L. Haack, D. VanDerveer, D. *J. Org. Chem.* **1980**, *45*, 1807–1817.
[30] H. Yokoi, Y. Hiraoka, S. Hiroto, D. Sakamaki, S. Seki, H. Shinokubo, *Nat. Commun.* **2015**, *6*, 8215.
[31] Deposition Number(s) <url href="https://www.ccdc.cam.ac.uk/services/structures?id=doi:10.1002/chem.20210XXX"> 2111840 (for **13**) </url> contain the supplementary crystallographic data for this paper. These data are provided free of charge by the joint Cambridge Crystallographic Data Centre and Fachinformationszentrum Karlsruhe <url href=" http://www.ccdc.cam.ac.uk/structures ">Access Structures service</url>.
[32] T. M. Krygowski, M. K. Cyrański, *Chem. Rev.* **2001**, *101*, 1385–1420.
[33] Z. Chen, C. S. Wannere, C. Corminboeuf, R. Puchta, P. v. R. Schleyer, *Chem. Rev.* **2005**, *105*, 3842–3888.
[34] H. Fallah-Bagher-Shaidaei, C. S. Wannere, C. Corminboeuf, R. Puchta, P. v. R. Schleyer, *Org. Lett.* **2006**, *8*, 863–866.
[35] D. Geuenich, K. Hess, F. Köhler, R. Herges, *Chem. Rev.* **2005**, *105*, 3758–3772.

Entry for the Table of Contents

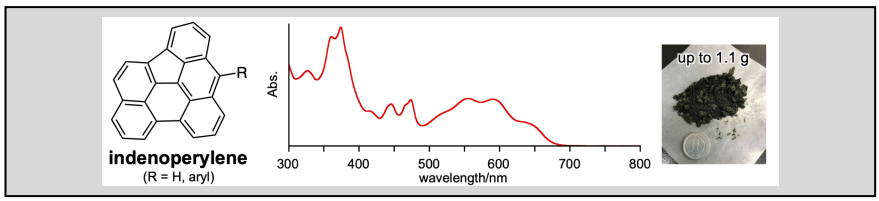

The synthesis and properties of indeno[1,2,3,4-*pqra*]perylene are described. Indenoperylene is a medium-sized aromatic hydrocarbon with the composition $C_{24}H_{12}$ that is isomeric to coronene. Nevertheless, its absorption covers the entire visible region owing to its small HOMO–LUMO gap. Furthermore, indenoperylene exhibits high stability despite the absence of peripheral substituents.

Institute and/or researcher Twitter usernames: @shinolab